Toxicological Sciences
ToxSci Advance Access published June 19, 2007

1073757

Internalization of Libby amphibole asbestos and induction of oxidative stress in murine macrophages

David J. Blake*, Celeste M. Bolin†, David P. Cox†, Fernando Cardozo-Pelaez† and Jean C. Pfau†

*Division of Biological Sciences** *and Department of Biomedical & Pharmaceutical Sciences, Center for Environmental Health Sciences†, University of Montana, Missoula, Montana, 59812*

Authors Email Addresses: david.blake@umontana.edu, celeste.bolin@umontana.edu, david.cox@umontana.edu, fernando.cardozo@umontana.edu, jean.pfau@umontana.edu

Corresponding Author Mailing Address: Center for Environmental Health Sciences, University of Montana, Missoula, Montana 59812.

Phone: (406) 243-4529. Fax: (406) 243-2807.

Email: jean.pfau@umontana.edu.

Short Title: Oxidative stress induced by Libby asbestos

Journal Section: Respiratory Toxicology

Abstract: The community members of Libby, Montana have experienced significant asbestos exposure and developed numerous asbestos related diseases (ARD) including fibrosis and lung cancer due to an asbestos contaminated vermiculite mine near the community. The form of asbestos in the contaminated vermiculite has been characterized in the amphibole family of fibers. However, the pathogenic effects of these fibers have not been previously characterized. The purpose of this study is to determine the cellular consequences of Libby amphibole exposure in macrophages compared to another well characterized amphibole fiber; crocidolite asbestos. Our results indicate that Libby asbestos fibers are internalized by macrophages and localize to the cytoplasm and cytoplasmic vacuoles similar to crocidolite fibers. Libby asbestos fiber internalization generates a significant increase in intracellular reactive oxygen species (ROS) as determined by DCFDA and DHE fluorescence indicating that the superoxide anion is the major contributing ROS generated by Libby asbestos. Elevated superoxide levels in macrophages exposed to Libby asbestos coincide with a significant suppression of total SOD activity. Both Libby and crocidolite asbestos generate oxidative stress in exposed macrophages by decreasing intracellular GSH levels. Interestingly crocidolite asbestos, but not Libby asbestos, induces significant DNA damage in macrophages. This study provides evidence that the difference in the level of DNA damage observed between Libby and crocidolite asbestos may be a combined consequence of the distinct chemical compositions of each fiber as well as the activation of separate cellular pathways during asbestos exposure.

Keywords: asbestos, Libby amphibole, murine macrophage, oxidative stress, DNA damage

Introduction

Asbestos exposure in humans is associated with the development of asbestos-related diseases (ARD) such as pulmonary fibrosis and lung cancer. Although the exact mechanism leading to the progression of ARD has not been fully explained, mounting evidence indicates that reactive oxygen species (ROS), such as the superoxide anion and the hydroxyl radical, play a significant role (Bhattacharya *et al.* 2005; Kamp and Weitzman 1999). Because airways are continuously exposed to high levels of environmental oxidants, they must maintain the proper balance between pro-oxidants and antioxidants to prevent oxidative stress and cellular damage. Environmental toxicants that alter the cellular redox state in the lung promote oxidative stress and lead to pulmonary injury. Oxidative stress is therefore associated with numerous pulmonary diseases including asthma, chronic obstructive pulmonary disease and pulmonary fibrosis (Rahman *et al.* 2006).

The vermiculite mine and surrounding community of Libby, Montana were designated as EPA Superfund sites in 2002 due to the asbestos contamination of vermiculite, which led to significant asbestos exposure throughout the mine site and surrounding area (Wright *et al.* 2002). The extensive asbestos exposure has led to considerable health problems in the community including reduced pulmonary function, enhanced autoimmune responses and increased mortality from lung cancer, malignant mesothelioma and fibrosis (McDonald *et al.* 2004; Pfau *et al.* 2005; Whitehouse 2004). The form of asbestos in Libby's contaminated vermiculite has been characterized in the amphibole family of fibers and consists of several hydrated silicate fibers, including regulated fibers (tremolite) and unregulated fibers (winchite and richterite) (Meeker *et al.*

2003). The regulated and unregulated fibers within Libby amphibole asbestos differ in terms of length and in the metallic cations expressed on their surface. Because of their diverse chemical composition Libby amphibole fibers are different from other well studied amphibole fibers, such as crocidolite and amosite, and therefore may induce distinct cellular effects in exposed cells.

Crocidolite asbestos generates an increase in ROS, which leads to a depletion of intracellular glutathione and oxidative damage to DNA and lipids in several cell types (Faux and Howden 1997; Fung *et al.* 1997; Golladay *et al.* 1997; Janssen *et al.* 1992; Kamp *et al.* 1992; Kim *et al.* 2001; Vallyathan *et al.* 1992; Xu *et al.* 2002; Yamaguchi *et al.* 1999). Moreover, ROS induced by crocidolite plays an important role in the activation of redox sensitive transcription factors such as NF-KB and AP-1 (Faux and Howden 1997; Flaherty *et al.* 2002). Because ROS generated by amphibole asbestos results in oxidative stress, the mechanism by which asbestos induces ROS production has been extensively studied. However, the exact source of ROS in response to asbestos fibers is an area of considerable debate and may be due to the unique chemical characteristics of the asbestos fiber (Kamp and Weitzman 1999).

Amphibole asbestos generates increased levels of ROS through at least two independent mechanisms. Amphibole asbestos fibers, specifically crocidolite and amosite, participate in the direct production of ROS via iron-catalyzed reactions due to their high iron content (Kamp and Weitzman 1999; Mossman and Gee 1997). This mechanism is supported by studies demonstrating that crocidolite asbestos cytotoxicity can be abrogated in the presence of iron chelators (Goodglick and Kane 1986). The importance of iron in asbestos fiber chemistry is also supported *in vivo* given the fact that

iron chelators protect against pulmonary inflammation and fibrosis (Kamp *et al.* 1995). The second proposed mechanism by which amphibole asbestos generates oxidative stress is through the production of mitochondrial-derived ROS. Alveolar epithelial cells generate intracellular ROS, which results in DNA damage and apoptosis in response to amosite asbestos (Panduri *et al.* 2006; Panduri *et al.* 2004).

The alveolar macrophage is the primary cell type that interacts with inhaled particles and functions to clear particles from the lung. Therefore, our study utilizes primary murine alveolar macrophages and a well characterized macrophage cell line. Our data indicate that Libby amphibole asbestos induces oxidative stress in murine macrophages through increasing ROS levels and suppressing SOD activity. The cellular effects of Libby asbestos exposure appear to be distinct from what is observed with crocidolite asbestos and may be a result of the activation of separate cellular mechanisms within exposed macrophages. This is the first study to elucidate the cellular changes in macrophages as a result of exposure to Libby amphibole asbestos.

Materials and Methods

Cell culture conditions

Mouse macrophages, RAW264.7 cells, (ATCC-2091: American Type Culture Collection, Manassas, VA) were cultured at 37°C in a 5% CO_2 incubator (Thermo Forma, Waltham, MA) in complete media, which contained DMEM media with 4.5 g/L glucose and L-glutamine supplemented with 1.5 mM sodium pyruvate, 20 mM HEPES, 55 µM 2-mercaptoethanol, 10% fetal bovine serum and antibiotics (100 U/ml penicillin, 100 µg/ml streptomycin and 0.25 µg/ml amphotericin B) (Gibco BRL, Bethesda, MD).

Confluent RAW264.7 cells were scraped from T75 flasks, counted with a Z series Coulter Counter (Beckman Coulter, Hialeah, FL) and plated into 96, 12 and 6 well plates or T75 flasks in complete media and allowed to adhere overnight prior to exposure to asbestos fibers. Primary alveolar macrophages were lavaged from C57BL/6 mice as previously described (Migliaccio *et al.* 2005), plated, and immediately exposed to asbestos. To elucidate the role of free radical scavengers, cells were incubated with superoxide dismutase (SOD) coupled to methoxypolyethylene glycol overnight at a final concentration of 19.6 Units (U) per ml (Sigma Chemical Co., St. Louis, MO) and concomitantly exposed to asbestos fibers. All experiments were performed using adherent cells only.

Particulate Matter

Three types of fibers were used in this study. Libby asbestos was obtained from the US Geological Survey. The Libby amphibole fibers have been chemically and physically characterized in detail (Gunter *et al.* 2003; Meeker *et al.* 2003; Wylie and Verkouteren 2000). The Libby asbestos sample is chemically representative of the amphibole in the mine and has a particle size distribution that matches the air sample size distribution data (Meeker *et al.* 2003). Libby asbestos contains six different amphibole fiber types, therefore, the asbestos sample is labeled in this paper as 6-mix. Wollastonite, a non-cytotoxic, non-fibrogenic control fiber, was provided by NYCO Minerals (Willsboro, NY). Crocidolite asbestos was provided by the Research Triangle Institute (RTI, NC). All fibers were dispersed in phosphate buffered saline (pH 7.4) by cup-horn sonication (Misonix, Framingdale, NY) before culturing. Stock concentration

suspensions of fibers were prepared fresh immediately prior to their addition into complete RPMI cell cultures. Fiber concentrations were based on relative mass. The size distributions of all three fiber types are presented in Table 1.

Transmission Electron Microscopy

RAW264.7 cells were exposed to Libby asbestos fibers at a concentration of 5 μg/cm^2 for 24 h. Cells were washed three times in PBS, detached with a cell scraper and fixed with 4% glutaraldehyde in PBS for 4 h at 25°C. Cells were centrifuged for 5 min at 5000 rpm, washed three times in PBS and the pellet was suspended in low melt agarose. The pellet was post-fixed in 1% osmium tetraoxide in PBS (pH 7.4) for 1 h at 25°C, and washed three times in PBS. The pellet was dehydrated in ethanol and embedded in resin. Ultrathin sections (50 nm) were examined under a Hitachi H-7100 transmission electron microscopy (Hitachi, Ibaraki, Japan) with a tungsten filament and captured with an Advanced Microscopy Techniques digital camera (AMT, Danvers, MA). Sections were viewed at 75 kV. Images were captured with the AMT software version 540.

Cell Viability

RAW264.7 cells were exposed to fiber concentrations and duration stated in the figures. Cells were incubated with trypsin-EDTA (Gibco BRL) for 5 min at room temperature. Complete media was added to stop the reaction. The cells were washed once and centrifuged at 1000 X g for 10 min. The pellet was resuspended in 200 μl of PBS to obtain a single cell suspension. Cells were permeabilized with 1 ml of 80% ethanol and incubated at -20°C overnight. Cells were washed once in PBS and DNA was stained with

1 ml of PBS containing 0.5% Triton X-100 (Sigma), 50 µg/ml RNase A (Roche, Indianapolis, IN) and 50 µg/ml propidium iodide (PI) (Invitrogen, Carlsbad, CA) then incubated for 40 min at 37°C. Cells were transferred to filter-top polypropylene tubes (BD Labware, Franklin Lakes, NJ) and stored on ice for analysis using the FACS Caliber (BD Biosciences, San Jose, CA) for red fluorescence. Dead and apoptotic cells were identified in the sub-G0/G1 peak determined by PI immunofluorescence. Cell viability was calculated as the percent of viable cells (cells above the sub-G0/G1 phase) divided by the total percent of cells and expressed as percent of control.

Cell viability of RAW264.7 cells after 3 h of exposure to Libby asbestos at a final concentration of 62.5 µg/cm^2 was not significantly different than controls as determined by a one-way ANOVA. These results were confirmed by an LDH-Cytotoxicity Assay (BioVision, Mountain View, CA) and the CellTiter-Blue Reagent assay (Promega, Madison, WI).

Enumeration of internalized fibers

Fiber uptake was quantified as previously described with slight modifications (Boylan *et al.* 1995). Briefly, RAW264.7 cells were exposed to Libby asbestos for 3 h at a final concentration of 62.5 µg/cm^2. Cells were washed with PBS and detached with trypsin-EDTA (Gibco) for 10 min with gentle rotation at RT to remove any fibers that were adherent but not internalized. Complete media was added to stop the reaction. The cells were washed in PBS and then examined under phase contrast microscopy to count the number of internalized fibers. The number of fibers per cell was quantified from 0 to 5. Greater than 5 fibers per cell were impossible to differentiate, therefore, the upper limit

of detection was 5 fibers per cell. Cells with more than 5 internalized fibers were classified into the upper limit (5). 50 cells in random fields were enumerated for each treatment. The experiment was performed twice with similar results.

Quantification of ROS in response to Libby amphibole asbestos

ROS production was measured using dichlorofluorescein diacetate (DCFDA, Molecular Probes, Eugene, OR) and dihydroethidine (DHE, Molecular Probes). DCFDA crosses the cell membrane and is trapped in the cell after deacetylation by intracellular esterases to dichlorofluorescin (DCFH). DCFH is then sensitive to oxidation, forming the fluorescent compound dichlorofluorecein (DCF) (Halliwell and Whiteman 2004). DHE is more specific for superoxide than DCFDA and is also oxidized to a fluorescent product (Zhao *et al.* 2003). Cells were plated in 96-well plates and incubated overnight at 37°C and 5% CO_2. Cells were incubated with 40 µM DCFDA for 1 hr or in 2 µM DHE for 30 min in a 37°C and 5% CO_2 incubator then exposed to fibers at concentrations stated in the figures. The plate was returned to the 37°C, 5% CO_2 incubator between hourly readings on the fluorescent plate reader. Cells without dye were used to subtract background fluorescence. Readings for fluorescence intensity were measured using a SpectraMax fluorescent plate reader set at 485 nm excitation and 530 nm emissions for DCFDA quantification and 518 nm excitation and 605 nm emission for DHE quantification (Molecular Devices, Sunnyvale, CA).

Quantification of total superoxide dismutase (SOD) activity

Total SOD activity was measured as described previously (Cardozo-Pelaez *et al.* 1998). Briefly, RAW264.7 cells were exposed to asbestos for 3, 7, 12 and 24 h at a final concentration of 62.5 µg/cm^2. The cells were washed with PBS and homogenized in 10 mM ethylenediaminetetraacetic acid disodium salt (EDTA) buffer (pH 8.0) by cup-horn sonication. Samples were centrifuged at 20,000 X g at 4°C for 15 min. The supernatants (15 µl) were incubated for 20 min in a 25°C water bath with 150 µl phosphate buffer, 15 µl of 1.5 mM xanthine, and 15 µl of 1.0 mM hydroxylamine chloride. The reaction was initiated by the addition of 75 µl of 0.8 mg protein/ml xanthine oxidase (Sigma). An aliquot of the reaction (100 µl) was added to a mixture of 100 µl of 19 mM sulfanilic acid and 100 µl of 7 mM α-napthylamine in a 96-well plate, incubated at room temperature for 20 min, and the absorbance was read at 539 nm using a SpectraMax plate reader (Molecular Devices). The activity of total SOD was determined from a standard curve using known amounts of purified SOD and quantified as Units of SOD activity per milligram of protein. Data are expressed as the percent of total SOD activity compared to time matched controls.

Quantification of reduced glutathione (GSH)

GSH levels were measured using the GSH recycling assay as previously described (Schneider *et al.* 2005). RAW264.7 cells were exposed to asbestos at concentrations and durations stated in the figures. The cells were washed with PBS and lysed with 2 freeze/thaw cycles in 300 µl of 10 mM HCl. 50 µl aliquots were taken for protein determination. Protein was precipitated by adding 70 µl of 6.5% sulfosalicylic acid, incubating on ice for 10 min and centrifuging at 2000 X g for 15 min. 200 µl of

supernatant was transferred to a 96-well plate for GSH quantification. Total intracellular glutathione was measured using the GSH reductase-DTNB recycling assay, comparing the rate of color formation at 412 nm of the unknowns to a standard curve. Total intracellular GSH levels were determined by quantifying the intracellular GSH levels and dividing by the protein concentration to obtain nmoles of GSH per milligram (mg) protein. Data are expressed as the percent of total glutathione levels compared to time matched controls.

Quantification of 8-hydroxy-2'-deoxyguanosine (8-oxo-dG)

RAW264.7 cells were exposed to asbestos for 12 and 24 h and 8-oxo-dG levels were quantified using the method previously described (Bolin *et al.* 2004). Briefly, DNA was isolated through phenol-chloroform extraction and digested with nuclease P1 (Roche). 8-oxo-dG and 2-deoxyguanosine (2dG) were resolved by HPLC with a reverse phase YMCBasic column (YMC Inc., Wilmington, NC) and quantified using a CoulArray electrochemical detection system (ESA Inc., Chelmsford, MA). Calibration curves were generated from standards of 2-dG (Sigma) ranging from 100 ng to 2 µg and 8-oxo-dG (Cayman Chemical, Ann Arbor, MI) ranging from 5 to 100 pg. The amount of 2-dG and 8-oxo-dG in control and treated cells was calculated according to the calibration curves. The relative levels of 8-oxo-2dG are expressed as the ratio of 8-oxo-2dG (fmoles) / 2dG (nmoles). Data were recorded, analyzed and stored using CoulArray for Windows data analysis software.

Determination of DNA damage

DNA damage was determined by the comet assay according to previously published methods with minor modifications (Tice *et al.* 1991). Briefly, 5ul of the cell suspension was embedded in 75 ul of 0.5% low melt agarose (Bio-Rad) and sandwiched between a layer of 5 ul of 0.5% normal melting agarose and a top layer of 0.5% low melting agarose on conventional microscope slides. To lyse cellular and nuclear membranes of the embedded cells, slides were immersed in ice-cold, freshly prepared, lysis solution (2.5 M NaCl, 100 mM disodium EDTA, 10 mM Tris-Cl and 10% DMSO, pH 13.0) and incubated at 4°C for 1 hour. The slides were incubated in alkaline buffer (0.1% 8-hydroxyquinoline, 10 mM disodium EDTA, 2% DMSO and 200 mM NaOH) for 20 min to allow DNA unwinding. Electrophoresis was performed in alkaline buffer at 300 mA for 20 min. After electrophoresis, the slides were neutralized with 400 mM Tris-Cl, pH 7.4 twice for 20 min. DNA was stained with 100 ul per slide of Hoechst (10 ug/ml) (Molecular Probes). All steps were conducted in darkness to prevent additional DNA damage and samples were analyzed within 4 h.

Microscopic analysis

A laser scanning cytometer (LSC, Compucyte, Cambridge, MA) equipped with a BX50 Olympus microscope and a 407-nm argon laser was used to scan the slides. Hoechst fluorescence was detected with a photomultiplier tube equipped with a 460-485 nm bandpass filter. The embedded cells were focused and scanned on the central portion of each well. The sensitivity threshold was set to contour comet heads only. A threshold value of greater than 3000 provided a good discrimination between nuclear fluorescence and comet tails. Fluorescence was integrated from a region of 6 pixels broader than the

threshold around the comet head as previously described (Petersen *et al.* 2000). For each integration contour, the integrated fluorescence, maximum pixel and the area were collected. The scanning was run by using a 20x dry objective. Two thousand events were scanned per slide. A histogram of integral fluorescence was compared to that obtained by flow cytometric cell cycle analysis through LSC software (WinCyte, Compucyte). The G1 and G2 phase peak were confirmed by LSC imaging. Cells with damaged DNA contained less DNA and stained with lower fluorescence intensity than the G1 phase cells and therefore appeared in the sub-G1 area of the histogram.

Quantification of 8-oxoguanine-DNA-glycosylase 1 (Ogg1) activity

RAW264.7 cells were exposed to asbestos for 3, 7 and 12 h and Ogg1 activity levels were quantified using the method previously described (Bolin *et al.* 2004). Briefly, DNA glycosylase was extracted from the pellets of the EDTA sample buffers, as described above, through homogenization at 4°C in extraction buffer containing 20 mM Trizma-base (pH 8.0), 1 mM EDTA, 0.5 mM spermine, 0.5 mM spermidine, 1 mM DTT, 50% glycerol, and protease inhibitor cocktail (Roche). Following the addition of 2.5 M potassium chloride, the homogenate was incubated at 4°C for 30 min. Aliquots of the supernatant were collected following centrifugation at 20,000 g for 30 min and stored at -80°C. Ogg1 activity was determined using a synthetic probe containing 8-oxo-dG (Trevigen, Gaithersburg, MD) labeled with γ-^{32}P at the 5'-end, using T4 polynucleotide kinase (Roche). The probe used has the nucleotide sequence 5'-GAACTAGTGXATCCCCCGGGCTGC-3' (X=8-oxo-dG) and was annealed to its corresponding complimentary oligonucleotide before the nicking reaction was preformed.

The nicking reaction was initiated by incubating 2.5 µg of protein extract and the double-stranded probe for 30 min at 37°C and stopped by placing the samples on ice. Aliquots of loading buffer containing 90% formamide, 10 mM NaOH and blue-orange dye (Promega, Madison, WI) were then added to each sample. After 5 min at 95°C, samples were chilled and loaded into a polyacrylamide gel (20%) with 7 M urea and 1X TBE and run at 400 V for 2 h. Gels were quantified using FLA-3000 Series Fuji Film Fluorescent Image Analyzer and analysis software. The capacity of the extract to remove 8-oxo-dG was expressed as a percentage of the cleaved synthetic probe to the total probe used in densitometric units.

Protein Determination

Protein concentrations were determined with the BCA protein assay kit based on the bicinchoninic acid (BCA) method (Pierce, Rockford, IL). The assay, adapted for microtiter plates, was used according to the manufacture's instructions.

Statistical Analysis

Data are given as mean ± standard deviation (SD) or mean ± standard error of the mean (SEM). Analyses were done using the software package GraphPad Prism 3.03 (GraphPad, San Diego, CA). One-way or two-way analysis of variance (ANOVA) was used to compare groups with one independent or two independent variables, respectively. A Bonferroni or Dunnett's post test was used to compare different treatments. Data comparing two group means were analyzed by independent samples *t* test. Significance was noted at $P < 0.05$ and adjusted for the number of comparisons according to

Bonferroni's adjustment. Non-parametric analysis of fiber uptake was conducted using the Kruskal-Wallis test. Outliers were detected through Grubb's test from GraphPad Software.

Results

Libby asbestos fibers are internalized by murine macrophages

To determine whether Libby asbestos fibers are internalized *in vitro*, murine macrophages were exposed to Libby asbestos at a concentration of 5 μg/cm^2 for 24 h and analyzed through transmission electron microscopy. After 24 h of asbestos exposure, murine macrophages contained variable numbers of asbestos fibers, which were less than 2 microns in length. The majority of Libby asbestos fibers were observed in cytoplasmic vacuoles or protruding from cytoplasmic vacuoles into the cytosol (Fig. 1A and B, respectively), and localized primarily around the nucleus. Libby asbestos fibers were also observed attached to the plasma membrane (Fig. 1C) and free within the cytoplasm (Fig. 1D). These results indicate that murine macrophages phagocytize Libby asbestos fibers and the internalized fibers localize to cytoplasmic vacuoles and to the cytosol.

Libby asbestos increases intracellular ROS in murine macrophages

To establish whether macrophages produce increased levels of ROS in response to amphibole asbestos, RAW264.7 cells were incubated with 40 μM DCFDA for one hour then exposed to increasing concentrations of Libby asbestos, ranging from 6.25 to 62.5 μg/cm^2. DCFDA is a fluorescent dye used to indirectly quantify the amount of intracellular ROS. Therefore, the relative fluorescence intensity is correlated to the

amount of intracellular ROS. Fluorescent readings were taken every hour for 3 h. The relative fluorescence intensities in macrophages over time are shown in Figure 2A. Murine macrophages increased intracellular ROS levels in response to Libby asbestos in a dose dependant manner. The lowest concentration of Libby asbestos (6.25 $\mu g/cm^2$) significantly increased the relative fluorescence after 3 h of exposure compared to untreated cells ($P < 0.05$). However, higher concentrations of Libby asbestos significantly increased the relative fluorescence after only one hour of exposure ($P < 0.05$). The highest concentration of Libby asbestos (62.5 $\mu g/cm^2$) generated the greatest increase in ROS and this concentration of asbestos did not reduce cell viability within 3 h as determined by PI immunofluorescence (Figure 2B) and two additional viability assays (see Materials and Methods). The viability of RAW264.7 cells after 3, 7, 12 and 24 h of exposure to Libby and crocidolite asbestos is shown in Figure 2B. The viability of RAW264.7 cells after 24 h of exposure to Libby and crocidolite asbestos was 92% and 62%, respectively, compared to untreated cells. Exposure to wollastonite fibers for 24 h did not reduce the viability of RAW264.7 cells compared to untreated controls (data not shown). Since the highest concentration of Libby asbestos induced the greatest increase in ROS without decreasing cell viability, we utilized this fiber concentration for all subsequent experiments.

In order to determine whether the increase in ROS was unique to Libby asbestos, murine macrophages were exposed to equal concentrations of Libby asbestos, wollastonite fibers, a non-fibrogenic control fiber (Tatrai *et al.* 2004), and a well characterized cytotoxic asbestos fiber, crocidolite. As shown in Figure 2C, cells exposed to Libby asbestos had a significantly higher relative fluorescence after only one hour of

exposure compared to untreated cells ($P < 0.05$). Exposure to wollastonite fibers did not increase the level of fluorescence in macrophages at any time during exposure compared to control cells. Cells exposed to crocidolite increased the level of fluorescence after 3 h of exposure; however, the increase in ROS was lesser in magnitude compared to Libby asbestos exposure. Similar results were obtained using primary alveolar macrophages lavaged from C57BL/6 mice (data not shown). These results demonstrate that exposure to Libby and crocidolite asbestos increases intracellular ROS in murine macrophages and the increase in intracellular ROS occurs in primary alveolar macrophages as well as in macrophage cell line cells.

Equivalent number of murine macrophages interact and internalize crocidolite and Libby asbestos fibers

To determine whether the increase in ROS was dependant upon the number of cell-fiber interactions or fiber uptake, we used light microscopy to enumerate the number of cells interacting with asbestos fibers and the number of internalized fibers per cell. To this end, murine macrophages were exposed to equal concentrations of Libby and crocidolite asbestos and wollastonite fibers for 3 h as described above. Cells were washed extensively and examined under phase contrast light microscopy. The number of cells interacting with one or more fibers where enumerated for each treatment. One hundred cells were counted for each treatment.

The preparation of Libby asbestos fibers contained numerous fibers of different lengths and widths. As seen in Figure 3A, Libby asbestos fibers visualized through light microscopy were generally less than 100 microns in length. Additionally, all murine

macrophages bound or internalized one or more Libby asbestos fibers after 3 h. The preparation of crocidolite asbestos was more homogeneous in morphology and contained longer fibers than the Libby asbestos. All murine macrophages also established multiple interactions with crocidolite asbestos fibers after 3 h (Fig 3B). Wollastonite fibers interacted with 25% of macrophages and had fewer fibers in each preparation compared to either amphibole asbestos preparations (Fig 3C). These results indicate that equal numbers of murine macrophages bind Libby and crocidolite asbestos fibers after 3 h at the concentrations used in this study.

The number of internalized fibers per cell was quantified as previously described with minor modifications (Boylan *et al.* 1995). On average, macrophages internalized 4.38 ± 1.06 Libby asbestos fibers per cell and 3.28 ± 1.58 crocidolite asbestos fibers per cell (mean ± SD). The difference between the numbers of Libby and crocidolite asbestos fibers internalized per cell was not significant. In contrast, macrophages internalized significantly fewer wollastonite fibers per cell (0.88 ± 0.93) compared to the number of amphibole asbestos fibers ($P < 0.05$). Together these data indicate that the increase in the level of ROS in macrophages is not dependent upon the number of cellular interactions with the asbestos fibers nor is it dependent on the number of internalized amphibole fibers.

Increased ROS levels generated by Libby asbestos is suppressed with the addition of exogenous intracellular SOD

To determine whether ROS induced by Libby amphibole asbestos can be inhibited by a free radical scavenger, RAW264.7 cells were incubated overnight with

SOD coupled to methoxypolyethylene glycol (PEG). SOD catalyzes the formation of hydrogen peroxide from superoxide anion and the conjugation of PEG leads to the enhanced uptake of exogenous SOD into cells (Beckman *et al.* 1988). After treatment with PEG-SOD, macrophages were washed and subsequently exposed to Libby asbestos, therefore, the effect of PEG-SOD on asbestos induced ROS production can only be attributed to intracellular SOD activity. As shown in Figure 4A, macrophages exposed to Libby asbestos had a significantly higher level of intracellular ROS after 3 h of asbestos exposure ($P < 0.05$). However, macrophages pretreated with PEG-SOD and subsequently exposed to Libby asbestos had significantly lower levels of intracellular ROS compared to macrophages exposed to asbestos alone ($P < 0.05$). Pretreatment of macrophages with PEG-SOD did not change the levels of ROS compared to control cells, indicating that the protective effect of PEG-SOD during asbestos exposure can be attributed to a reduction in superoxide levels. Pretreatment of cells with PEG alone did not inhibit ROS produced by Libby asbestos (data not shown). These data confirm that Libby asbestos induced ROS is predominately intracellular and can be abrogated by PEG-SOD, suggesting that the superoxide anion is the major contributor to the increased ROS levels.

Libby asbestos increases superoxide production in murine macrophages

To provide additional support for the premise that a contributing ROS generated by Libby amphibole asbestos is the superoxide anion, RAW264.7 cells were incubated with 2 µM DHE for 30 min then exposed to Libby asbestos at a final concentration of 62.5 µg/cm^2. DHE is a fluorescent dye used to indirectly quantify the amount of superoxide in cells. Therefore, the relative fluorescent intensity is correlated to

intracellular superoxide levels (Zhao *et al.* 2003). The relative DHE fluorescence intensity of murine macrophages exposed to Libby asbestos and wollastonite fibers is shown in Figure 4B. Macrophages exposed to Libby asbestos had a significantly higher relative fluorescence after 2 h of exposure compared to untreated cells ($P < 0.05$). Macrophages exposed to wollastonite fibers did not increase the level of fluorescence compared to control. These data indicate that Libby asbestos exposure increases intracellular levels of superoxide in murine macrophages.

Total intracellular SOD activity is suppressed by Libby amphibole asbestos

Because Libby asbestos exposure increases superoxide levels in murine macrophages, we hypothesized that the increase in superoxide may be due to a modification in SOD activity. Therefore, total intracellular SOD activity was quantified in murine macrophages after 3, 7, 12 and 24 h of exposure as previously described (Cardozo-Pelaez *et al.* 1998). Libby asbestos suppressed total SOD activity by 30% after 3 h of exposure and the reduction in activity was significant compared to untreated controls ($P < 0.05$) (Fig 5). However, total SOD activity was not significantly different compared to controls after 7, 12 and 24 h of exposure to Libby asbestos. Total SOD activity was not different in cells exposed to wollastonite compared to time matched controls. Crocidolite asbestos significantly increased total SOD activity by 200% after 24 h of exposure compared to untreated controls ($P < 0.05$). These results indicate that exposure to Libby asbestos results in an initial suppression of total SOD activity and that exposure to crocidolite asbestos increases total SOD activity after 24 h in murine macrophages.

Intracellular glutathione levels are reduced in response to Libby amphibole asbestos

In response to increased levels of ROS, cells utilize GSH to maintain the intracellular redox balance within cells. Reduced levels of intracellular GSH in cells are an indication of oxidative stress. Therefore, intracellular GSH was measured in macrophages after exposure to amphibole asbestos and wollastonite fibers to determine whether exposure results in a decrease in intracellular GSH levels. The intracellular GSH levels were measured through the GSH recycling assay as previously described (Schneider *et al.* 2005). In response to Libby asbestos, macrophages significantly decreased intracellular GSH levels compared to untreated cells at 7, 12 and 24 h ($P < 0.05$) (Fig. 6). Exposure to crocidolite asbestos also significantly decreased intracellular GSH levels at 7, 12 and 24 h after exposure. However, the decrease in GSH levels was more prominent in response to crocidolite asbestos (average decrease of 55%) at all time points compared to the decrease observed with Libby asbestos (average decrease of 76%). Wollastonite did not decrease the intracellular GSH levels compared to time matched controls. These results indicate that exposure to Libby and crocidolite asbestos induces oxidative stress in murine macrophages.

Libby amphibole does not promote the formation of 8-oxo-dG or single stranded DNA breaks in macrophages

RAW264.7 cells were exposed to Libby asbestos, crocidolite asbestos and wollastonite fibers and the relative levels of 8-oxo-dG were determined as previously described (Bolin *et al.* 2004) in order to determine whether the increased levels of ROS

generated by Libby and crocidolite asbestos results in oxidative DNA damage. The relative level of 8-oxo-dG is quantified as a ratio of 8-oxo-dG compared to deoxyguanosine. Only adherent cells were included in the DNA damage assay. The levels of 8-oxo-dG in macrophages were significantly elevated in response to crocidolite asbestos at 12 and 24 hr ($P < 0.05$) (Fig. 7A). However, in the same cell type, Libby asbestos did not increase the relative levels of 8-oxo-dG at either time 12 or 24 h. Wollastonite, did not increase the relative levels of 8-oxo-dG at either 12 or 24 h. In response to Libby and crocidolite asbestos, the extent of DNA damage, specifically strand breaks, was also quantified at 24 h through the comet assay (Fig. 7B). Crocidolite asbestos generated a significantly higher level of DNA damage as determined by the percent of cells in the sub-G1 phase ($P < 0.05$). Libby amphibole did not produce a significant difference in the percentage of cells in the sub-G1 phase. These data indicate that Libby asbestos does not induce oxidative DNA damage in murine macrophage cells and suggests Libby asbestos induces separate cellular responses *in vitro* compared to crocidolite asbestos.

Effect of Libby asbestos on Ogg1 activity

Ogg1 is an important DNA glycosylase/AP lyase that catalyzes the excision of 8-oxo-dG lesions from damaged DNA and its activity has been shown to increase during oxidative stress (Sava *et al.* 2004). To determine whether the lack of DNA damage with Libby asbestos was a result of increased DNA repair generated by asbestos-induced oxidative stress, the activity of Ogg1 was quantified as previously described (Bolin *et al.* 2004). Murine macrophages were exposed to fibers for 12 and 24 h and the activity of

Ogg1 was quantified as the percent of cleaved synthetic oligonucleotide, which contains an 8-oxo-dG residue, compared to the total amount of oligonucleotide. As seen in Figure 7C, the activity of Ogg1 in macrophages exposed to Libby asbestos and wollastonite fibers was not different at either time point compared to untreated control cells. Exposure to crocidolite asbestos induces a significant increase in Ogg1 activity in murine macrophages after 12 h, however, Ogg1 activity returns to control levels after 24 h. These results indicate that exposure to Libby asbestos does not increase the activity of Ogg1 in murine macrophages.

Discussion

The community members of Libby, MT have experienced significant exposure to amphibole asbestos and have developed numerous ARD due to the asbestos contaminated vermiculite mine near the community (McDonald *et al.* 2004; Whitehouse 2004). The type of amphibole fiber that residents have been exposed to is a distinct type of amphibole asbestos, which is composed of several different fiber types (Meeker *et al.* 2003). Because this asbestos type has not been previously studied, we determined the cellular effects of these fibers in order to elucidate a possible cellular mechanism for the initiation of ARD. Our study utilized a phagocytic cell line that is characteristic of alveolar macrophages as well as primary alveolar macrophages that interact and clear inhaled particles in the lung (Xia *et al.* 2006).

Our data indicate that macrophages internalize Libby asbestos fibers and that the fibers localize to the cytosol and to cytoplasmic vacuoles that frequently surround the nucleus. These data are in accordance with previous results that establish crocidolite

fibers are internalized through a microtubule dependant mechanism and localize near the nucleus (Cole *et al.* 1991). The majority of internalized Libby asbestos fibers are 2 microns or less in length. Libby asbestos fibers of this size have been shown to accumulate in the bark of trees throughout the mine site and surrounding area, indicating these size fibers are respirable and persist in the environment (Ward *et al.* 2006). These short, thin fibers are also the predominant asbestos fibers that remain in the tissue of asbestos exposed humans with pleural plaques and malignant mesothelioma (Suzuki *et al.* 2005). Hence, these size fibers play an important role in the development of fibrosis and lung cancer (Dodson *et al.* 2003).

Exposure to Libby asbestos increases the level of intracellular ROS in murine macrophages and can be significantly reduced by exogenous PEG-SOD. These results suggest that the superoxide anion contributes to ROS generated by Libby asbestos exposure. To support the argument that superoxide contributes to asbestos induced ROS, Libby asbestos exposure also increases DHE fluorescence. DHE is known to preferentially detect superoxide (Zhao *et al.* 2003). Together these data indicate that Libby asbestos exposure increases intracellular ROS levels in macrophages and that the major contributing ROS is the superoxide anion.

We hypothesized that the increase in superoxide may be due to an alteration of antioxidant concentrations within exposed cells. Therefore, intracellular SOD activity was quantified with an assay that measures total SOD activity and cannot differentiate between the activity of intracellular copper-zinc SOD and mitochondrial manganese SOD. Exposure to Libby asbestos causes a significant decrease in total SOD activity after 3 h of exposure. The decrease in total SOD activity would consequently generate the

observed increase in superoxide levels due to Libby asbestos exposure. The reduction in SOD activity by Libby asbestos may be due to post-translational modifications of SOD as a result of fiber internalization (Marks-Konczalik *et al.* 1998). In contrast, crocidolite asbestos increases total SOD activity after 24 h, which has been previously reported in mesothelial cells (Cardinali *et al.* 2006). Chronic exposure to crocidolite asbestos has also been shown to increase SOD activity *in vivo* and *in vitro* (Janssen *et al.* 1992; Mossman *et al.* 1986). SOD is highly expressed in cells within the lung, such as alveolar macrophages (Kinnula and Crapo 2003). The increased SOD activity observed during amphibole exposure may be a protective antioxidant response in response to the increased levels of free radicals generated by amphibole internalization.

Exposure to Libby asbestos results in an increase in ROS in conjunction with a significant decrease in intracellular GSH. The decrease in GSH with Libby asbestos was most notable after 7 h and remained significantly decreased after 24 h of exposure. Crocidolite also significantly decreased GSH levels after 7 h of exposure. These data are in accordance with previously published results that indicate crocidolite asbestos exposure results in a significant decrease in intracellular GSH level in both mesothelial and epithelial cells (Golladay *et al.* 1997; Janssen *et al.* 1995). In the present study, crocidolite asbestos induces a greater decrease in GSH levels than Libby asbestos, which coupled with the increased cytotoxicity of this fiber, correlates to a higher level of oxidative stress in RAW264.7 cells (Xiao *et al.* 2003).

Unlike previous studies that utilize only a single amphibole fiber, this study utilizes a sample of Libby asbestos that is a mixture of several amphiboles as well as other fibers not classified in the amphibole family (Meeker *et al.* 2003). Although

exposure to Libby asbestos generates increased levels of ROS, no DNA damage was observed. In contrast, crocidolite asbestos exposure significantly increases DNA damage, which supports previous reports (Fung *et al.* 1997; Kim *et al.* 2001). The lack of DNA damage observed with Libby asbestos may be a result of increased DNA repair activity in cells exposed to Libby asbestos. The main defense against oxidative DNA damage is the base excision repair pathway, which is initiated by Ogg1. The activity of Ogg1 significantly increases in murine macrophages in response to crocidolite asbestos, which supports previous *in vitro* results in alveolar epithelial cells (Kim *et al.* 2001). However, no difference in Ogg1 activity was observed after exposure to Libby asbestos. Therefore the lack of DNA damage in macrophages in response to Libby asbestos cannot be explained by increased DNA repair activity in these cells.

Although crocidolite and Libby asbestos are both categorized as amphibole fibers, they are chemically distinct. The major difference between these two fibers is that crocidolite contains a high iron content that is greater than 20% (Kamp and Weitzman 1999). The high iron content is known to play a role in crocidolite induced DNA damage (Mossman and Gee 1997; Xu *et al.* 2002). On the contrary, Libby amphibole contains less than 5% iron content by weight (Meeker *et al.* 2003). In addition to differences in chemical composition, this study describes separate cellular consequences of each fiber in the same cell line. DNA damage observed with crocidolite asbestos may be an indirect result of the increased SOD activity observed after 24 h (Figure 8). Increased SOD activity produces excess hydrogen peroxide from the dismutation of superoxide. Increased levels of hydrogen peroxide in crocidolite exposed macrophages may interact with the iron associated with crocidolite asbestos fibers and promote the formation of the

hydroxyl radical. Indeed crocidolite fibers have been shown to promote the formation of the hydroxyl radical in the presence of hydrogen peroxide (Kamp *et al.* 1992; Kamp and Weitzman 1999). The hydroxyl radical is the most oxidizing ROS in biological systems and promotes the oxidation of 2-dG in DNA generating 8-oxo-dG, which is observed in macrophages in response to crocidolite asbestos (Figure 7A) (Buettner 1993). In contrast, Libby asbestos suppresses total SOD activity in macrophages and generates the production of superoxide in exposed cells. The observation that Libby asbestos does not induce DNA damage, may be due to the fact that superoxide has a considerably lower reduction potential and does not participate in the oxidation of 2-dG. Therefore, we hypothesize that the differences in DNA damage observed among Libby and crocidolite asbestos may be a combined consequence of the distinct chemical compositions of each fiber as well as the activation of separate cellular pathways during asbestos exposure (Figure 8).

In summary, murine macrophages phagocytize Libby amphibole asbestos fibers, which localize to the cytoplasm and cytoplasmic vacuoles. Internalization of Libby asbestos results in an increase in ROS levels, which can be attributed to the suppression of total SOD activity observed subsequent to Libby asbestos exposure. These results are in contrast to what is observed with crocidolite asbestos, which induces oxidative DNA damage. These data support the premise that the cellular effects observed with different asbestos fibers are mediated by their chemical compositions and the activation of separate cellular mechanisms. Finally, this is the first study to characterize the cellular effects Libby amphibole asbestos, a pathogenic fiber known to cause ARD in humans.

Acknowledgements

The authors thank Ray Hamilton and Sandra Wells, Center for Environmental Health Sciences, University of Montana and James S. Webber, Wadsworth Center, NY for helpful discussions, Pamela Shaw in the CEHS Fluorescence Cytometry Core for assistance with the FACS analysis and Anna Marie Ristich, Microscopy Section Manager, at DataChem Laboratories for assistance with the fiber analysis.

Grants

This work was funded by grants from the NIH P20 NCRR017670 and R21 ES012956.

References

Beckman, J. S., Minor, R. L., Jr., White, C. W., Repine, J. E., Rosen, G. M., and Freeman, B. A. (1988). Superoxide dismutase and catalase conjugated to polyethylene glycol increases endothelial enzyme activity and oxidant resistance. *J Biol Chem* **263**, 6884-92.

Bhattacharya, K., Dopp, E., Kakkar, P., Jaffery, F. N., Schiffmann, D., Jaurand, M. C., Rahman, I., and Rahman, Q. (2005). Biomarkers in risk assessment of asbestos exposure. *Mutat Res* **579**, 6-21.

Bolin, C., Stedeford, T., and Cardozo-Pelaez, F. (2004). Single extraction protocol for the analysis of 8-hydroxy-2'-deoxyguanosine (oxo8dG) and the associated activity of 8-oxoguanine DNA glycosylase. *J Neurosci Methods* **136**, 69-76.

Boylan, A. M., Sanan, D. A., Sheppard, D., and Broaddus, V. C. (1995). Vitronectin enhances internalization of crocidolite asbestos by rabbit pleural mesothelial cells via the integrin alpha v beta 5. *J Clin Invest* **96**, 1987-2001.

Buettner, G. R. (1993). The pecking order of free radicals and antioxidants: lipid peroxidation, alpha-tocopherol, and ascorbate. *Arch Biochem Biophys* **300**, 535-43.

Cardinali, G., Kovacs, D., Maresca, V., Flori, E., Dell'Anna, M. L., Campopiano, A., Casciardi, S., Spagnoli, G., Torrisi, M. R., and Picardo, M. (2006). Differential in vitro cellular response induced by exposure to synthetic vitreous fibers (SVFs) and asbestos crocidolite fibers. *Exp Mol Pathol* **81**, 31-41.

Cardozo-Pelaez, F., Song, S., Parthasarathy, A., Epstein, C. J., and Sanchez-Ramos, J. (1998). Attenuation of age-dependent oxidative damage to DNA and protein in brainstem of Tg Cu/Zn SOD mice. *Neurobiol Aging* **19**, 311-6.

Cole, R. W., Ault, J. G., Hayden, J. H., and Rieder, C. L. (1991). Crocidolite asbestos fibers undergo size-dependent microtubule-mediated transport after endocytosis in vertebrate lung epithelial cells. *Cancer Res* **51**, 4942-7.

Dodson, R. F., Atkinson, M. A., and Levin, J. L. (2003). Asbestos fiber length as related to potential pathogenicity: a critical review. *Am J Ind Med* **44**, 291-7.

Faux, S. P., and Howden, P. J. (1997). Possible role of lipid peroxidation in the induction of NF-kappa B and AP-1 in RFL-6 cells by crocidolite asbestos: evidence following protection by vitamin E. *Environ Health Perspect* **105 Suppl 5**, 1127-30.

Flaherty, D. M., Monick, M. M., Carter, A. B., Peterson, M. W., and Hunninghake, G. W. (2002). Oxidant-mediated increases in redox factor-1 nuclear protein and activator protein-1 DNA binding in asbestos-treated macrophages. *J Immunol* **168**, 5675-81.

Fung, H., Kow, Y. W., Van Houten, B., and Mossman, B. T. (1997). Patterns of 8-hydroxydeoxyguanosine formation in DNA and indications of oxidative stress in rat and human pleural mesothelial cells after exposure to crocidolite asbestos. *Carcinogenesis* **18**, 825-32.

Golladay, S. A., Park, S. H., and Aust, A. E. (1997). Efflux of reduced glutathione after exposure of human lung epithelial cells to crocidolite asbestos. *Environ Health Perspect* **105 Suppl 5**, 1273-7.

Goodglick, L. A., and Kane, A. B. (1986). Role of reactive oxygen metabolites in crocidolite asbestos toxicity to mouse macrophages. *Cancer Res* **46**, 5558-66.

Gunter, M. E., Dyar, D. M., Twamley, B., Foit Jr, F. F., and Cornelius, S. (2003). Composition, Fe+3/Fe and crystal structure of non-asbestiform and asestiform amphiboles from Libby, Montana, USA. *American Mineralogist* **89**, 1579.

Halliwell, B., and Whiteman, M. (2004). Measuring reactive species and oxidative damage in vivo and in cell culture: how should you do it and what do the results mean? *Br J Pharmacol* **142**, 231-55.

Janssen, Y. M., Heintz, N. H., and Mossman, B. T. (1995). Induction of c-fos and c-jun proto-oncogene expression by asbestos is ameliorated by N-acetyl-L-cysteine in mesothelial cells. *Cancer Res* **55**, 2085-9.

Janssen, Y. M., Marsh, J. P., Absher, M. P., Hemenway, D., Vacek, P. M., Leslie, K. O., Borm, P. J., and Mossman, B. T. (1992). Expression of antioxidant enzymes in rat lungs after inhalation of asbestos or silica. *J Biol Chem* **267**, 10625-30.

Kamp, D. W., Graceffa, P., Pryor, W. A., and Weitzman, S. A. (1992). The role of free radicals in asbestos-induced diseases. *Free Radic Biol Med* **12**, 293-315.

Kamp, D. W., Israbian, V. A., Yeldandi, A. V., Panos, R. J., Graceffa, P., and Weitzman, S. A. (1995). Phytic acid, an iron chelator, attenuates pulmonary inflammation and fibrosis in rats after intratracheal instillation of asbestos. *Toxicol Pathol* **23**, 689-95.

Kamp, D. W., and Weitzman, S. A. (1999). The molecular basis of asbestos induced lung injury. *Thorax* **54**, 638-52.

Kim, H. N., Morimoto, Y., Tsuda, T., Ootsuyama, Y., Hirohashi, M., Hirano, T., Tanaka, I., Lim, Y., Yun, I. G., and Kasai, H. (2001). Changes in DNA 8-hydroxyguanine levels, 8-hydroxyguanine repair activity, and hOGG1 and hMTH1 mRNA expression in human lung alveolar epithelial cells induced by crocidolite asbestos. *Carcinogenesis* **22**, 265-9.

Kinnula, V. L., and Crapo, J. D. (2003). Superoxide dismutases in the lung and human lung diseases. *Am J Respir Crit Care Med* **167**, 1600-19.

Marks-Konczalik, J., Gillissen, A., Jaworska, M., Loseke, S., Voss, B., Fisseler-Eckhoff, A., Schmitz, I., and Schultze-Werninghaus, G. (1998). Induction of manganese superoxide dismutase gene expression in bronchoepithelial cells after rockwool exposure. *Lung* **176**, 165-80.

McDonald, J. C., Harris, J., and Armstrong, B. (2004). Mortality in a cohort of vermiculite miners exposed to fibrous amphibole in Libby, Montana. *Occup Environ Med* **61**, 363-6.

Meeker, G. P., Bern, A. M., Brownfield, I. K., Lowers, H. A., Sutley, S. J., Hoefen, T. M., and Vance, J. S. (2003). The Composition and Morphology of Amphiboles from the Rainy Creek Complex, Near Libby, Montana. *American Mineralogist* **88**, 1955-1969.

Migliaccio, C. T., Hamilton, R. F., Jr., and Holian, A. (2005). Increase in a distinct pulmonary macrophage subset possessing an antigen-presenting cell phenotype and in vitro APC activity following silica exposure. *Toxicol Appl Pharmacol* **205**, 168-76.

Mossman, B. T., and Gee, J. B. (1997). Asbestos-related cancer and the amphibole hypothesis. The hypothesis is still supported by scientists and scientific data. *Am J Public Health* **87**, 689-90; author reply 690-1.

Mossman, B. T., Marsh, J. P., and Shatos, M. A. (1986). Alteration of superoxide dismutase activity in tracheal epithelial cells by asbestos and inhibition of cytotoxicity by antioxidants. *Lab Invest* **54**, 204-12.

Panduri, V., Surapureddi, S., Soberanes, S., Weitzman, S. A., Chandel, N., and Kamp, D. W. (2006). P53 mediates amosite asbestos-induced alveolar epithelial cell mitochondria-regulated apoptosis. *Am J Respir Cell Mol Biol* **34**, 443-52.

Panduri, V., Weitzman, S. A., Chandel, N. S., and Kamp, D. W. (2004). Mitochondrial-derived free radicals mediate asbestos-induced alveolar epithelial cell apoptosis. *Am J Physiol Lung Cell Mol Physiol* **286**, L1220-7.

Petersen, A. B., Gniadecki, R., and Wulf, H. C. (2000). Laser scanning cytometry for comet assay analysis. *Cytometry* **39**, 10-5.

Pfau, J. C., Sentissi, J. J., Weller, G., and Putnam, E. A. (2005). Assessment of autoimmune responses associated with asbestos exposure in Libby, Montana, USA. *Environ Health Perspect* **113**, 25-30.

Rahman, I., Biswas, S. K., and Kode, A. (2006). Oxidant and antioxidant balance in the airways and airway diseases. *Eur J Pharmacol* **533**, 222-39.

Sava, V., Mosquera, D., Song, S., Cardozo-Pelaez, F., and Sanchez-Ramos, J. R. (2004). Effects of melanin and manganese on DNA damage and repair in PC12-derived neurons. *Free Radic Biol Med* **36**, 1144-54.

Schneider, J. C., Card, G. L., Pfau, J. C., and Holian, A. (2005). Air pollution particulate SRM 1648 causes oxidative stress in RAW 264.7 macrophages leading to production of prostaglandin E2, a potential Th2 mediator. *Inhal Toxicol* **17**, 871-7.

Suzuki, Y., Yuen, S. R., and Ashley, R. (2005). Short, thin asbestos fibers contribute to the development of human malignant mesothelioma: pathological evidence. *Int J Hyg Environ Health* **208**, 201-10.

Tatrai, E., Kovacikova, Z., Brozik, M., and Six, E. (2004). Pulmonary toxicity of wollastonite in vivo and in vitro. *J Appl Toxicol* **24**, 147-54.

Tice, R. R., Andrews, P. W., Hirai, O., and Singh, N. P. (1991). The single cell gel (SCG) assay: an electrophoretic technique for the detection of DNA damage in individual cells. *Adv Exp Med Biol* **283**, 157-64.

Vallyathan, V., Mega, J. F., Shi, X., and Dalal, N. S. (1992). Enhanced generation of free radicals from phagocytes induced by mineral dusts. *Am J Respir Cell Mol Biol* **6**, 404-13.

Ward, T. J., Spear, T., Hart, J., Noonan, C., Holian, A., Getman, M., and Webber, J. S. (2006). Trees as reservoirs for amphibole fibers in Libby, Montana. *Sci Total Environ* **367**, 460-5.

Whitehouse, A. C. (2004). Asbestos-related pleural disease due to tremolite associated with progressive loss of lung function: serial observations in 123 miners, family members, and residents of Libby, Montana. *Am J Ind Med* **46**, 219-25.

Wright, R. S., Abraham, J. L., Harber, P., Burnett, B. R., Morris, P., and West, P. (2002). Fatal asbestosis 50 years after brief high intensity exposure in a vermiculite expansion plant. *Am J Respir Crit Care Med* **165**, 1145-9.

Wylie, A. G., and Verkouteren, J. R. (2000). Amphibole asbestos from Libby, Montana, aspects of nomenclature. *American Mineralogist* **85**, 1540-1542.

Xia, T., Kovochich, M., Brant, J., Hotze, M., Sempf, J., Oberley, T., Sioutas, C., Yeh, J. I., Wiesner, M. R., and Nel, A. E. (2006). Comparison of the abilities of ambient and manufactured nanoparticles to induce cellular toxicity according to an oxidative stress paradigm. *Nano Lett* **6**, 1794-807.

Xiao, G. G., Wang, M., Li, N., Loo, J. A., and Nel, A. E. (2003). Use of proteomics to demonstrate a hierarchical oxidative stress response to diesel exhaust particle chemicals in a macrophage cell line. *J Biol Chem* **278**, 50781-90.

Xu, A., Zhou, H., Yu, D. Z., and Hei, T. K. (2002). Mechanisms of the genotoxicity of crocidolite asbestos in mammalian cells: implication from mutation patterns induced by reactive oxygen species. *Environ Health Perspect* **110**, 1003-8.

Yamaguchi, R., Hirano, T., Ootsuyama, Y., Asami, S., Tsurudome, Y., Fukada, S., Yamato, H., Tsuda, T., Tanaka, I., and Kasai, H. (1999). Increased 8-hydroxyguanine in DNA and its repair activity in hamster and rat lung after intratracheal instillation of crocidolite asbestos. *Jpn J Cancer Res* **90**, 505-9.

Zhao, H., Kalivendi, S., Zhang, H., Joseph, J., Nithipatikom, K., Vasquez-Vivar, J., and Kalyanaraman, B. (2003). Superoxide reacts with hydroethidine but forms a fluorescent product that is distinctly different from ethidium: potential implications in intracellular fluorescence detection of superoxide. *Free Radic Biol Med* **34**, 1359-68.

Table 1: Fiber size distribution data of Libby and crocidolite asbestos and wollastonite fibers

Fiber Type	Diameter (microns)	Length (microns)	Aspect Ratio
6-mix	0.61 ± 1.22	7.21 ± 7.01	22.52 ± 22.87
Crocidolite	0.16 ± 0.09	4.59 ± 4.22	34.05 ± 43.29
Wollastonite	0.75 ± 1.02	4.46 ± 5.53	8.48 ± 7.10

Note: Data are means ± SD.

Figure 1: Transmission electron microscopy of intracellular Libby asbestos fibers in murine macrophages. RAW264.7 cells were incubated with Libby asbestos (5 µg/cm^2) for 24 h and sections were prepared as described in Materials and Methods. A) Libby asbestos fiber is encompassed by a cytoplasmic vacuole near the nuclear membrane. Magnification 40,000X. B) Libby asbestos fiber near the nuclear membrane protruding from a cytoplasmic vacuole to the cytoplasm. Magnification 60,000X. C) Libby asbestos fibers attached to the plasma membrane. Magnification 15,000X. D) Libby asbestos fiber free in the cytosol of a murine macrophage. Magnification 30,000X. Double arrows denote the nuclear membrane. Single arrows denote the plasma membrane.

Figure 2: Dose-dependant response of Libby asbestos on intracellular ROS levels in RAW264.7 cells. ROS levels were determined by the relative fluorescence units (RFU) of DCFDA as described in Material and Methods. A) Three separate concentrations of Libby asbestos were added to murine macrophages for 3 h. Closed circles denote control cells. Open diamonds denote cells treated with Libby asbestos (6.25 µg/cm^2). Closed diamonds denote cells treated with Libby asbestos (32.25 µg/cm^2). Closed triangles denote cells treated with Libby asbestos (62.5 µg/cm^2). B) RAW264.7 cells were exposed to Libby and crocidolite asbestos for 3, 7 12 and 24 h. Cell viability was determined through PI fluorescence as described in Materials and Methods. Viability was calculated as the percent of viable cells (cells above the sub-G0/G1 phase) and expressed as a percent of control. Closed triangles denote cells treated with Libby asbestos (62.5 µg/cm^2). Closed diamonds denote cells treated with crocidolite (62.5 µg/cm^2). C) Separate experiment comparing Libby asbestos with wollastonite, a non-fibrogenic

control fiber, and crocidolite, a well-characterized cytotoxic fiber. Closed circles denote control cells. Closed rectangles denote cells treated with wollastonite (62.5 µg/cm^2). Closed triangles denote cells treated with Libby asbestos (62.5 µg/cm^2). Closed diamonds denote cells treated with crocidolite (62.5 µg/cm^2). Data are represented as mean ± SD. Single asterisks indicate a significant difference compared to control at each time point through a Bonferonni post-hoc test ($P < 0.05$; n = 3-5) by a two-way ANOVA.

Figure 3: Light microscopy of murine macrophages interacting with asbestos and non-asbestos fibers. RAW264.7 cells were incubated with Libby asbestos, crocidolite asbestos and wollastonite fibers at a final concentration of 62.5 µg/cm^2 for 3 h and visualized through phase contrast light microscopy. All RAW264.7 cells bound one or more Libby and crocidolite asbestos fibers (A and B, respectively) while wollastonite fibers interacted with fewer RAW264.7 cells (C). Scale bar = 100 microns.

Figure 4: Increase in superoxide levels in asbestos exposed macrophages. A) Effect of intracellular superoxide dismutase (SOD) on asbestos-induced ROS in RAW264.7 cells. Cells were incubated overnight at 37°C with SOD conjugated to methoxypolyethylene glycol (11.0 U/ml). Cells were then treated with Libby asbestos (62.5 µg/cm^2). ROS levels were determined by the RFU of DCFDA as described in Material and Methods. Open bars denote control cells. Thatched bars denote control cells pretreated overnight with PEG-SOD (44 U/ml). Black bars denote cells treated with Libby asbestos (62.5 µg/cm^2). Checkered bars denote cells pretreated overnight with PEG-SOD then exposed to Libby asbestos. B) Superoxide levels were determined by the RFU of DHE over 2 h as

described in Material and Methods. Open bars denote control cells. Black bars denote cells treated with Libby asbestos (62.5 µg/cm^2). Thatched bars denote cells treated with wollastonite (62.5 µg/cm^2). Data are represented as mean ± SEM. Single asterisks indicate a significant difference through a Bonferonni post-hoc test ($P < 0.05$; $n = 5$) by a one-way ANOVA.

Figure 5: Effect of Libby amphibole asbestos on total intracellular SOD activity in RAW264.7 cells. RAW264.7 cells were exposed to fibers as described in Materials and Methods for 3, 7, 12 and 24 h. Total SOD activity levels were quantified as a ratio of Units of SOD activity per mg of protein as previously described (Cardozo-Pelaez *et al.* 1998) and expressed as the percentage of total SOD activity compared to time matched controls. Open bars denote control cells. Thatched bars denote cells treated with wollastonite (62.5 µg/cm^2). Black bars denote cells treated with Libby asbestos (62.5 µg/cm^2). Checkered bars denote cells treated with crocidolite (62.5 µg/cm^2). Data are represented as mean ± SEM. Single asterisks indicate a significant difference compared to time matched controls through an independent *t* test ($P < 0.05$; $n = 4$).

Figure 6: Effect of amphibole asbestos on total intracellular glutathione levels in RAW264.7 cells. RAW264.7 cells were exposed to fibers as described in Materials and Methods. GSH levels were quantified as a ratio of GSH in nmoles per mg of protein as previously described (Schneider *et al.* 2005) and expressed as the percentage of total glutathione levels compared to time matched controls. Open bars denote control cells. Thatched bars denote cells treated with wollastonite (62.5 µg/cm^2). Black bars denote

cells treated with Libby asbestos (62.5 µg/cm^2). Checkered bars denote cells treated with crocidolite (62.5 µg/cm^2). Data are represented as mean ± SEM. Single asterisks indicate a significant difference compared to time matched controls through an independent *t* test ($P < 0.05$; $n = 3$).

Figure 7: Effect of amphibole asbestos on 8-dihydro-8-oxo-2'-deoxyguanosine (8-oxo-dG) levels and Ogg1 activity in RAW264.7 cells. A) RAW264.7 cells were exposed to asbestos as described in Materials and Methods for 12 h and 24 h. The relative levels of 8-oxo-dG in RAW264.7 cells were quantified as previously described (Bolin *et al.* 2004). The relative level of 8-oxo-dG is calculated as a ratio of 8-oxo-dG compared to 2-deoxyguanosine (2dG). Open bars denote control cells. Thatched bars denote cells treated with wollastonite (62.5 µg/cm^2). Black bars denote cells treated with Libby asbestos (62.5 µg/cm^2). Checkered bars denote cells treated with crocidolite (62.5 µg/cm^2). B) RAW264.7 cells were exposed to amphibole asbestos for 24 h and the percentage of cells that contained damaged DNA, which appeared in the sub-G1 peak, was quantified through the comet assay as described in Materials and Methods. Open bars denote control cells. Black bars denote cells treated with Libby asbestos (62.5 ug/cm^2). Checkered bars denote cells treated with crocidolite asbestos (62.5 ug/cm^2). Single asterisks indicate a significant difference compared to control by Dunnett's test ($P < 0.05$; $n = 4$). C) RAW264.7 cells were exposed to asbestos as described in Materials and Methods for 12 and 24 h. The activity levels of Ogg1 in cells were quantified as the percent of cleaved oligonucleotide as previously described (Bolin *et al.* 2004). Closed circles denote control cells. Closed rectangles denote cells treated with wollastonite (62.5 µg/cm^2). Closed

triangles denote cells treated with Libby asbestos (62.5 μg/cm^2). Closed diamonds denote cells treated with crocidolite (62.5 μg/cm^2). Data are represented as mean ± SEM. Single asterisks indicate a significant difference compared to control by Dunnett's test ($P < 0.05$; $n = 4$).

Figure 8: Schematic of the proposed mechanisms for Libby and crocidolite asbestos exposure. Internalization of Libby (labeled 6-mix) and crocidolite asbestos generate oxidative stress in RAW264.7 cells through increasing ROS levels and decreasing intracellular GSH levels. Libby asbestos suppresses SOD activity leading to the formation of superoxide ($O_2^{\bullet-}$). Crocidolite asbestos increases SOD activity, which generates hydrogen peroxide (H_2O_2). Hydrogen peroxide can then react with the iron (Fe II) associated with crocidolite fibers to from the reactive hydroxyl radical (OH•), which oxidizes 2-deoxyguanosine (2dG) to 8-hydroxy-2'-deoxyguanosine (8-oxo-dG) in murine macrophages.

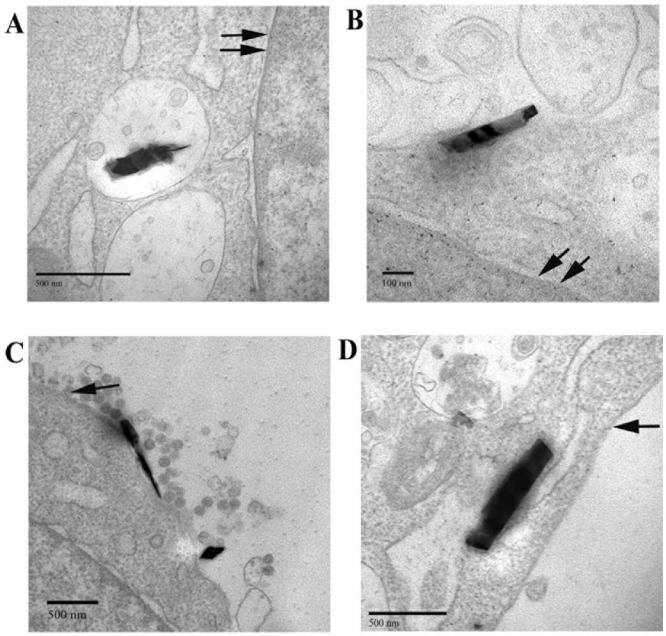

203x254mm (300 x 300 DPI)

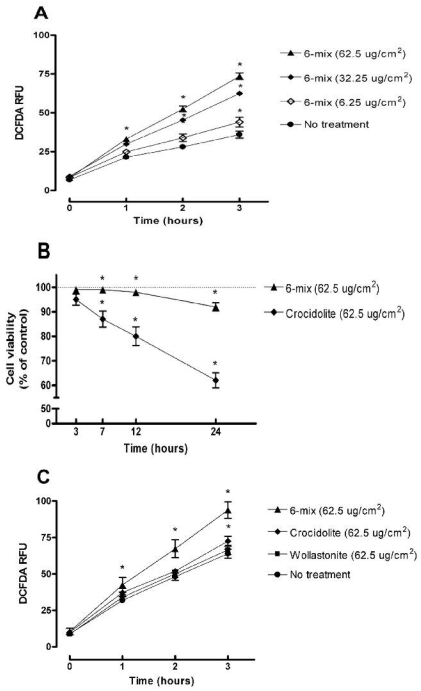

203x254mm (600 x 600 DPI)

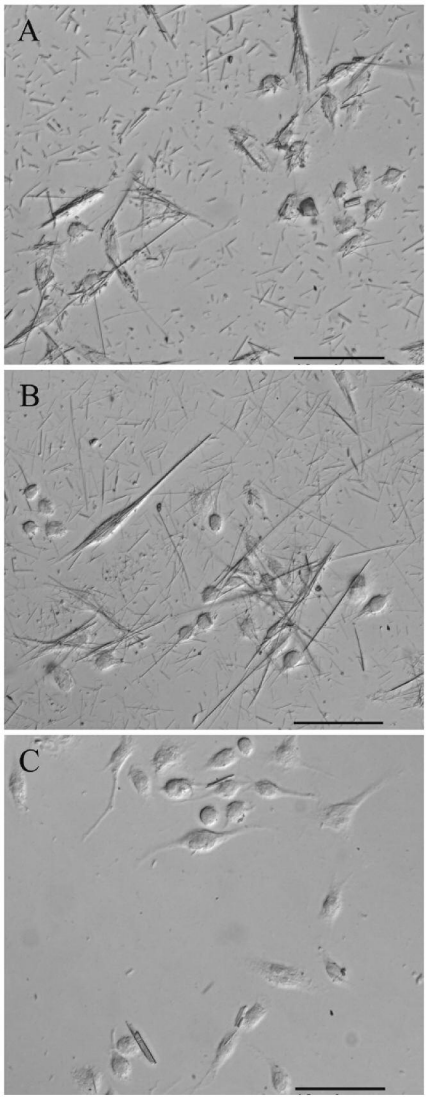

203x254mm (300 x 300 DPI)

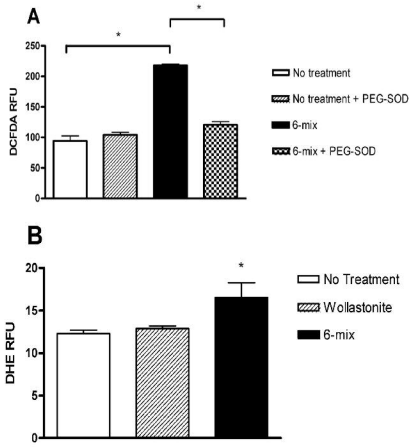

203x254mm (600 x 600 DPI)

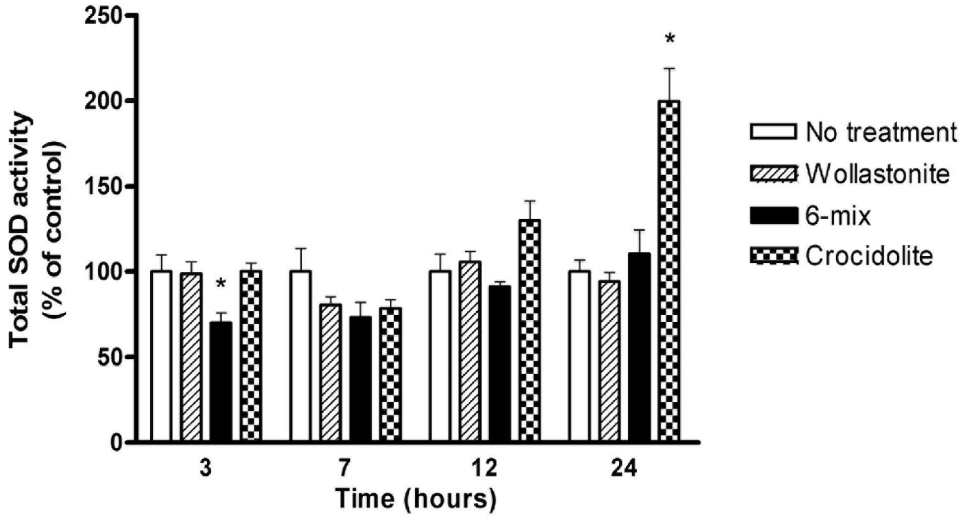

88x50mm (600 x 600 DPI)

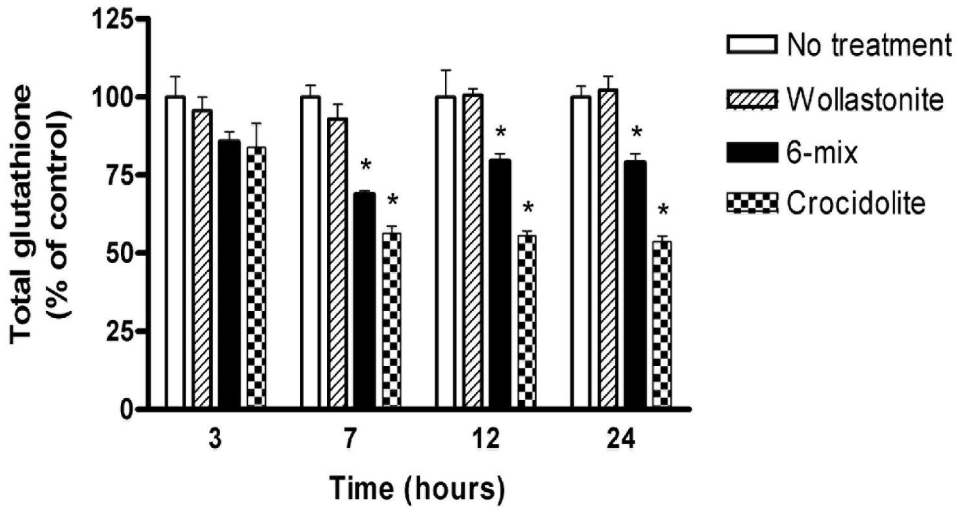

88x50mm (600 x 600 DPI)

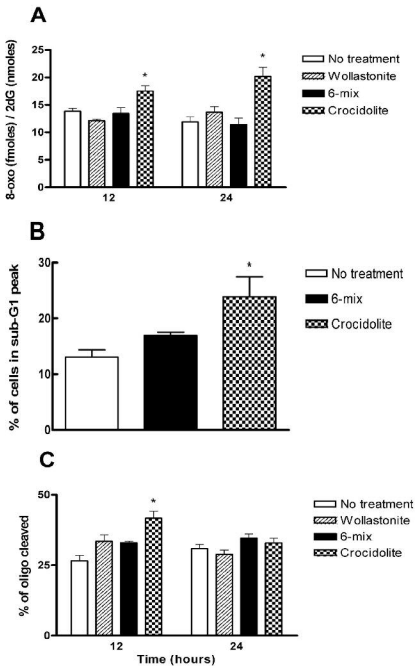

203x254mm (600 x 600 DPI)

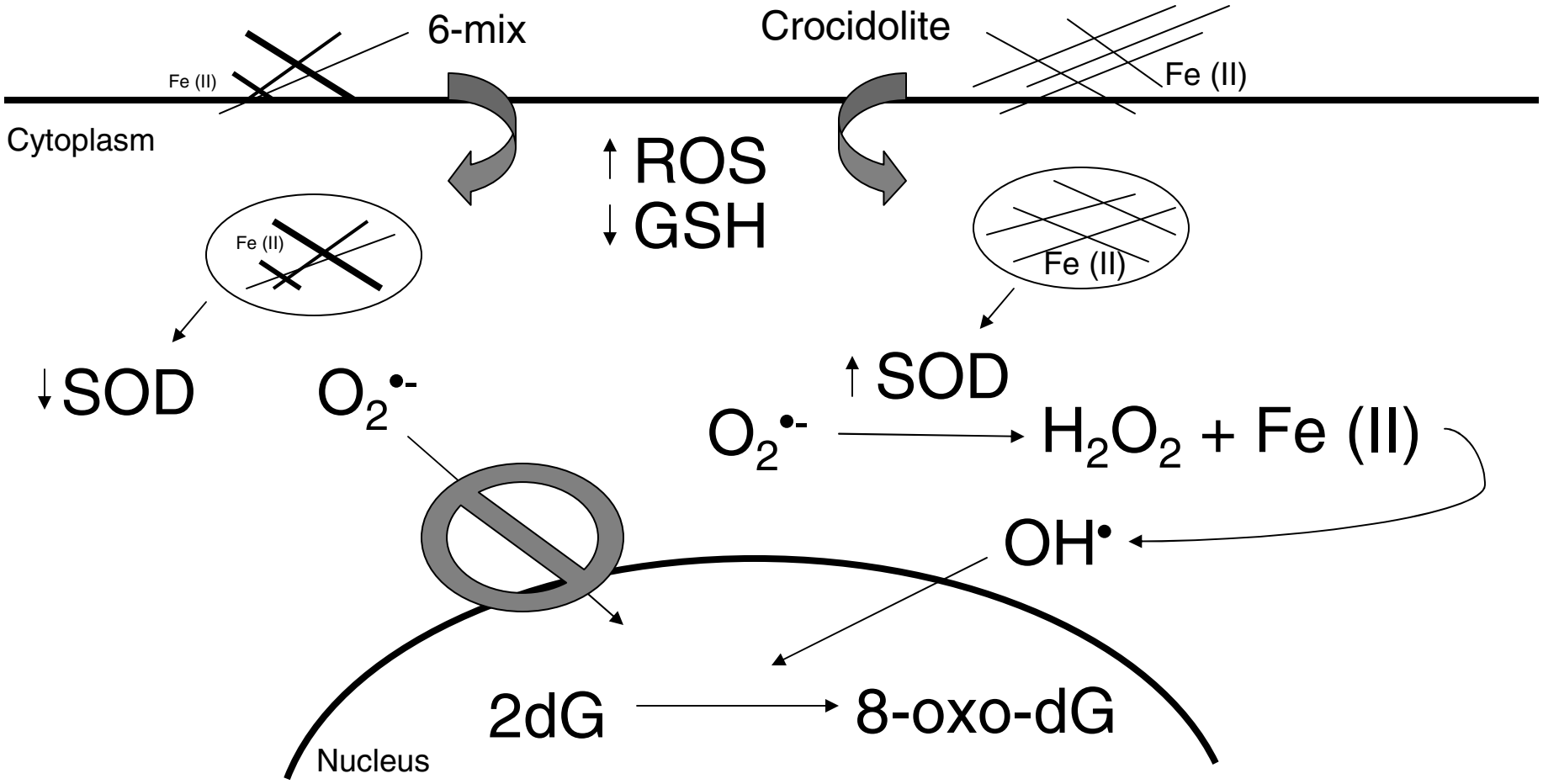
6-mix
Crocidolite
Fe (II)
Fe (II)
Cytoplasm
↑ ROS
↓ GSH
Fe (II)
Fe (II)
↓ SOD
$O_2^{\bullet-}$
↑ SOD
$O_2^{\bullet-}$
H_2O_2 + Fe (II)
$OH^{\bullet}$
2dG
8-oxo-dG
Nucleus